Brain, Behavior, & Immunity - Health 38 (2024) 100795

Contents lists available at ScienceDirect

Brain, Behavior, & Immunity - Health

journal homepage: www.editorialmanager.com/bbih/default.aspx

Trait-anxiety and glial-related neuroinflammation of the amygdala and its associated regions in Alzheimer's disease: A significant correlation

Fumihiko Yasuno [a,b,*], Yasuyuki Kimura [a,b], Aya Ogata [b,c], Hiroshi Ikenuma [b], Junichiro Abe [b], Hiroyuki Minami [a], Takashi Nihashi [a], Kastunori Yokoi [a], Saori Hattori [b], Nobuyoshi Shimoda [d], Atsushi Watanabe [e], Kensaku Kasuga [f], Takeshi Ikeuchi [f], Akinori Takeda [a], Takashi Sakurai [a], Kengo Ito [a,b], Takashi Kato [a,b]

[a] National Hospital for Geriatric Medicine, National Center for Geriatrics and Gerontology, Obu, Japan
[b] Department of Clinical and Experimental Neuroimaging, Center for Development of Advanced Medicine for Dementia, National Center for Geriatrics and Gerontology, Obu, Japan
[c] Department of Pharmacy, Faculty of Pharmacy, Gifu University of Medical Science, Kani, Japan
[d] Functional Genomics Unit, Medical Genome Center, National Center for Geriatrics and Gerontology, Obu, Japan
[e] Equipment Management Division, Center for Core Facility Administration, National Center for Geriatrics and Gerontology, Obu, Japan
[f] Department of Molecular Genetics, Brain Research Institute, Niigata University, Niigata, Japan

ARTICLE INFO

Keywords:
Alzheimer's disease
Positron emission tomography (PET)
Inflammation
State-Trait Anxiety Inventory (STAI)
Anxiety
amygdala

ABSTRACT

Background: Positron emission tomography, which assesses the binding of translocator protein radiotracers, ^{11}C-DPA-713, may be a sensitive method for determining glial-mediated neuroinflammation levels. This study investigated the relationship between regional ^{11}C-DPA713 binding potential (BP_{ND}) and anxiety in patients with Alzheimer's disease (AD) continuum.

Methods: Nineteen patients with AD continuum determined to be amyloid-/p-tau 181-positive via cerebrospinal fluid analysis were included in this cross-sectional study (mild cognitive impairment [MCI, n = 5] and AD [n = 14]). Anxiety was evaluated using the State-Trait Anxiety Inventory (STAI). A whole-brain voxel-based analysis was performed to examine the relationship between ^{11}C-DPA-713-BP_{ND} values at each voxel and the STAI score. Stepwise multiple regression analysis was performed to determine the predictors of STAI scores using independent variables, including ^{11}C-DPA-713-BP_{ND} values within significant clusters. ^{11}C-DPA-713-BP_{ND} values were compared between patients with AD continuum with low-to-moderate and high STAI scores.

Results: Voxel-based analysis revealed a positive correlation between trait anxiety severity and ^{11}C-DPA713-BP_{ND} values in the centromedial amygdala and the left inferior occipital area [$P < 0.001$ (uncorrected) at the voxel-level]. ^{11}C-DPA713-BP_{ND} values in these regions were a strong predictor of the STAI trait anxiety score. Specifically, patients with AD continuum and high trait anxiety had increased ^{11}C-DPA713-BP_{ND} values in these regions.

Conclusions: The amygdala–occipital lobe circuit influences the control of emotional generation, and disruption of this network by AD pathology-induced inflammation may contribute to the expression of anxiety. Our findings suggest that suppression of inflammation can help effectively treat anxiety by attenuating damage to the amygdala and its associated areas.

1. Introduction

Clinically, anxiety in Alzheimer's disease (AD) is often viewed as a component of a broader disorder, such as psychosis or depression, or as a symptom of other behaviors, particularly agitation and aggression (Mintzer and Brawman-Mintzer, 1996). Nevertheless, anxiety has been identified as a distinct symptom as well in patients with AD (Mega et al., 1996). A study of 523 community-dwelling patients with AD reported

* Corresponding author. National Hospital for Geriatric Medicine, National Center for Geriatrics and Gerontology, 7-430 Morioka-cho, Obu, Aichi, 474-8511, Japan.
E-mail address: yasunof@ncgg.go.jp (F. Yasuno).

https://doi.org/10.1016/j.bbih.2024.100795
Received 24 February 2024; Received in revised form 28 April 2024; Accepted 12 May 2024
Available online 14 May 2024

the prevalence of anxiety in 70% of the participants (Teri et al., 1999). A meta-analysis reported a pooled prevalence of 39% for anxiety in AD, with generalized anxiety disorder (GAD), characterized by persistent and excessive worry about various things, being the most common condition (Zhao et al., 2016).

An in-depth understanding of the neurobiological basis and neural pathways underlying anxiety in AD is essential for developing targeted interventions. A systematic review and meta-analysis that investigated the correlation between anxiety and two neuropathological markers in AD, namely, amyloid-beta (Aβ) and tau pathology, did not find any association between anxiety and these two markers (Demnitz-King et al., 2023). A sensitivity analysis evaluating anxiety type (i.e., characteristics and status) and biomarker assessment modality (i.e., positron emission tomography [PET] and cerebrospinal fluid [CSF]) did not find significant differences (Demnitz-King et al., 2023). Further research should investigate additional neurobiological factors to augment current knowledge of the correlation between anxiety and dementia.

Neuroinflammation contributes to AD development and its pathogenesis to the same extent as the neuropathological signs (Calsolaro and Edison, 2016; Heneka et al., 2015; Mhatre et al., 2015; Yasuno et al., 2023). Dysregulated neuroinflammation can result in the accumulation of inflammatory mediators and the activation of potentially neurotoxic resident immune cells, particularly microglia and astrocytes. This dysregulated neuroinflammation, in turn, can alter the structure, excitability, and connectivity of the corticolimbic network, which controls emotions (Fulton et al., 2022). It can be assumed that AD pathology-induced inflammatory response disrupts neural activity in the brain regions responsible for emotion processing, which triggers anxiety-like behavior. Studies have suggested a link between neuroinflammation and the pathology of anxiety-like behaviors in rodents (Liu et al., 2018; Wang et al., 2018). Therefore, understanding the connection between neuroinflammation and anxiety and identifying the underlying mechanisms of AD are vital for providing optimal treatment.

Glial cells such as microglia and astrocytes have crucial roles in inflammatory response (Heneka et al., 2015). Neuron damage activates microglia and astrocytes. PET-based visualization of activated glial cells in the brain may be useful for investigating the role of neuroinflammation in disease progression. The 18 kDa translocator protein (TSPO) is predominantly located in the mitochondrial outer membrane (Banati et al., 2004) and serves as an indicator of the burden of inflammatory responses. Its concentration increases in response to glial activation under pathological conditions. In vivo, PET imaging of glial-mediated neuroinflammation is possible using a radioactive tracer that binds to TSPO.

It has been hypothesized that the relationship between glia-mediated neuroinflammation and anxiety may be observable in the brain regions involved in fear, anxiety, and emotion processing, such as the amygdala and its associated areas. This hypothesis highlights the potential of maladaptive glia-mediated neuroinflammation reduction as a treatment strategy for anxiety-like behaviors in AD. However, to date, no in vivo TSPO-PET studies with the region of interest (ROI) based analysis identified a link between AD pathology-induced glial-mediated inflammation and changes in the brain regions associated with anxiety and emotional processing. Therefore, this study investigated the relationship between regional neuroinflammation and anxiety in patients with amyloid-positive AD continuum using TSPO-PET imaging with ^{11}C-DPA-713 as the radiotracer and a whole-brain voxel-wise analysis.

2. Material and methods

2.1. Participants

Among 23 patients with AD continuum who had TSPO–PET imaging data and were determined to be amyloid-/p-tau 181-positive via CSF analysis, 19 patients (mild cognitive impairment [MCI, n = 5] and AD [n = 14]) were included in this cross-sectional study. These patients were assessed for anxiety using the State-Trait Anxiety Inventory (STAI) (Spielberger et al., 1983). Four patients were excluded from the study as their anxiety could not be assessed using the STAI. The inclusion criteria for patients with MCI were as follows: Mini-Mental State Examination (MMSE) scores 24–30, objective memory loss, Clinical Dementia Rating (CDR) = 0.5, and preservation of basic activities of daily living. Probable AD was diagnosed according to the National Institute on Aging and Alzheimer's Association clinical criteria (McKhann et al., 2011) and MMSE scores <24. No patients were treated with anti-dementia drugs for AD at the examination.

Patients' CSF samples were stored at −80 °C at the biobank of the National Center for Geriatrics and Gerontology (NCGG). Amyloid and p-tau 181 positivity were determined by analyzing the CSF Aβ42/40 ratio and p-tau 181 concentrations, respectively, at the Brain Research Institute of Niigata University. The cutoff values for amyloid and p-tau 181 positivity were <0.072 (Kasuga et al., 2023) and >30.6 pg/mL (Kasuga et al., 2022), respectively, based on CSF samples from the Japanese Alzheimer's Disease Neuroimaging Initiative. The apolipoprotein E4 (ApoE4) genotype was determined via DNA analysis and polymerase chain reaction (Hixson and Vernier, 1990). Based on the rs6971 polymorphism within *TSPO*, all patients were classified as having high-affinity binders (Owen et al., 2011).

The Institutional Review Board of the National Center for Geriatrics and Gerontology approved this study. Written informed consent was obtained from all study participants.

2.2. STAI measures

Anxiety levels were evaluated using the STAI. The STAI comprises two segments: the State Anxiety Scale (STAI-S) and the Trait Anxiety Scale (STAI-T). The STAI-S measures transient anxiety states via questions on subjective emotions, such as nervousness, worry, tension, and fear. The STAI-T measures relatively stable aspects of anxiety tendencies and general states of calm, confidence, and security. Each scale contains 20 questions to be answered on a 4-point Likert scale. The overall results range from 20 to 80 for each scale, with higher scores indicating higher anxiety levels. Scores between 20 and 30 are classified as "no or low anxiety," those between 31 and 44 as "medium anxiety," and those between 45 and 80 as "high anxiety" (Bogavac et al., 2023).

2.3. PET image acquisition and analysis

The details of the PET image acquisition and analysis have been previously described (Yasuno et al., 2022).

Among the second-generation TSPO radiotracers with high target affinity, we used ^{11}C-DPA-713 for TSPO-PET imaging for two reasons: (1) A comparison study of TSPO tracers using a blocking agent found that DPA-713 had the highest binding potential in humans among PK11195, PBR28, DPA-713, and ER176, indicating that it had the best signal-to-noise ratio (Fujita et al., 2017). Although these authors observed that DPA-713 radio-metabolites entered the brain, they also found that quantification was only affected in participants with the low-affinity binding genotype and not in those with the high-affinity binding genotype, which all patients in the current study are. (2) In a previous study, we demonstrated that the non-displaceable binding potential of DPA-713 could be stably estimated using the Braak 6 area as the reference region (Yasuno et al., 2022).

Patients underwent 3D PET imaging (Biograph True V; Siemens Healthcare, Erlangen, Germany) 0–60 min after a bolus intravenous injection of 404.9 ± 40.8 MBq of ^{11}C-DPA-713 (range, 251–446 MBq). The mean ± standard deviation (SD) of the administered ^{11}C-DPA-713 was 5.9 ± 2.0 nmol (range, 2.9–10.5 nmol). The time bins within the 60 min period were 6 × 10 s, 3 × 20 s, 2 × 60 s, 2 × 180 s, and 10 × 300 s. Arterial blood samples were manually collected. Their radioactive concentrations were measured 12 times during the initial 2 min post-injection, 14 times during the subsequent 28 min, and once every 15

min until the end of the scan. Subsequently, time-radioactivity curves for whole blood and plasma were plotted based on measured radioactivity. Radiometabolite analysis of arterial blood samples manually collected at 5, 15, 30, 45, and 60 min was performed using a radio-high-performance liquid chromatography system (Prominence LC-20 system, Shimazu, Kyoto, Japan, and FC-4100, Eckert & Ziegler Radiopharma, Hopkinton, MA, USA). The arterial input functions of the parent radioactivity in plasma were created by correcting the plasma radioactivity using ligand metabolism.

The PET images were corrected for scattering, attenuation, and time-of-flight and reconstructed using the ordered subset expectation maximization method. The final reconstructed images comprised 109 planes of 168 × 168 voxels, measuring 2.04 × 2.04 × 2.03 mm^3. Dynamic PET images were corrected for motion and registered to the standard Montreal Neurological Institute (MNI) space using P-mod View and Registration and Fusion tools (PMOD Technologies, Zurich, Switzerland). Frame-by-frame motion correction was performed via the rigid-body registration of adjacent frames. Subsequently, the PET images were spatially normalized in the MNI stereotactic space using the parameters obtained from the transformation of the individual 3D-T1 MR images and a ROI template from the Automated Anatomical Labeling (AAL) atlas (Tzourio-Mazoyer et al., 2002), was applied.

Regional radioactivity was quantified in the ROIs that approximated the pathological Braak neurofibrillary tangle deposition stages anatomically (Braak and Braak, 1991). We calculated the time-activity curves from the composite ROI in the AAL atlas corresponding to the anatomical definitions of Braak stages 1–3 area (hippocampal and parahippocampal region, amygdala, lingual area, and fusiform area) (109.43 cm^3) as a target region, where the tangle deposition was expected at the stage of MCI and mild-to-moderate AD. Moreover, the stage 6 area (precentral area, calcarine area, cuneus area, postcentral area, and paracentral lobule) (191.01 cm^3) was used as the reference region, which was indicated as a non-target of ^{11}C-DPA-713 in mild-to-moderate AD previously (Yasuno et al., 2022).

The PET images were analyzed using the graphical Logan method with a metabolite-corrected plasma input function on a voxel-wise basis. This analysis produced a parametric image of the binding potential (BP_{ND}) using the following formula:

$$(V_T^{\ tissue} - V_T^{\ ref})/V_T^{\ ref}$$

, where $V_T^{\ tissue}$ and $V_T^{\ ref}$ are the total volume distribution of the target and reference tissues, respectively. The mean ± SD of $V_T^{\ ref}$ values of 19 patients is 10.3 ± 3.3, while that of $V_T^{\ tissue}$ values is 11.6 ± 3.6 in Braak stages 1–3.

2.4. Statistical analysis

Voxel-based analysis was performed to investigate the correlation between ^{11}C-DPA-713-BP_{ND} values at each voxel and the STAI-S and STAI-T scores and CSF Aβ42/40 ratio and CSF p-tau 181. The Statistical Parametric Mapping (SPM) 12 software was used for the analysis. The ^{11}C-DPA-713-BP_{ND} images were smoothed with a Gaussian kernel of 12 mm full-width at half-maximum.

For whole-brain analysis, statistical maps were thresholded at $P < 0.001$ (uncorrected) at the voxel level and $P < 0.05$ (familywise error (FWE)-corrected) at the cluster level. For brain regions with a hypothesized relationship between neuroinflammation and anxiety, such as the amygdala and its associated regions, less strict statistical thresholds were applied, with the voxel-level at $P < 0.001$ (uncorrected) and a minimum cluster size of $k \geq 100$, based on the expected voxels per cluster computed according to the random field theory (Hayasaka and Nichols, 2004). Subsequently, the regional ^{11}C-DPA-713-BP_{ND} values were calculated by averaging the values for all voxels within the significant clusters.

Voxel-based morphometric (VBM) analyses were performed using the MATLAB-based Computational Anatomy Toolbox (CAT12, http://dbm.neuro.uni-jena.de/cat/), which is an extension of SPM12 (Ashburner and Friston, 2000) to determine structural changes in the significant clusters in the above-described analysis. Structural images were corrected for bias-field inhomogeneity and registered using linear (12-parameter affine) and non-linear transformations. Tissue classification into gray matter (GM), WM, and CSF was performed within the same generative model (Ashburner and Friston, 2005). GM images were modulated to account for volume changes based on the normalization process. Images were spatially normalized into the stereotactic space of the Montreal Neurological Institute (MNI) and smoothed with a 6 mm (FWHM) Gaussian kernel (final voxel size: 1 mm × 1 mm × 1 mm). Further analyses were restricted to voxels with an *a priori* GM probability of >0.1 to avoid borderline effects between GM and WM. Mean VBM signals (gray matter voxel intensity) were calculated in the significant clusters shown in the voxel-based correlation analysis.

A stepwise multiple linear regression analysis was performed to identify the predictors of STAI-S and/or STAI-T scores that were found to be related to ^{11}C-DPA-713-BP_{ND} values in the voxel-based analysis. A stepwise backward-selection model was used. The STAI-T and/or STAI-S scores of each patient were measured as dependent variables. The independent variables included age, sex, years of education, ApoE4 positivity, CSF Aβ42/40 ratio, p-tau 181 concentration, and regional ^{11}C-DPA-713-BP_{ND} values within significant clusters. Significant clusters found in the same bilateral brain areas were combined to avoid multicollinearity.

A Bayesian multiple regression analysis was performed to overcome the limitations of stepwise model selection and sample size constraints of using advanced methods (e.g., regularized model fitting) and secure the robustness of our findings and reliance on our null results (Malpetti et al., 2020). Bayes factor (BF_{10}) was calculated for each model relative to the null model; $BF_{10} > 1$, $BF_{10} > 3$, $BF_{10} > 10$, and $BF_{10} > 100$ indicated weak/anecdotal, substantial, strong, and decisive evidence for a relationship (against the null hypothesis), respectively (Kass and Raftery, 1995).

^{11}C-DPA713-BP_{ND} values within significant clusters were compared between patients with AD continuum with low-to-moderate (<45) and high (>45) STAI scores (Bogavac et al., 2023) using multivariate analysis of covariance (MANCOVA) with covariates of variables mentioned as predictors of STAI score in multiple regression analysis.

Stepwise multiple linear regression, Spearman's correlation analysis, and MANCOVA were performed using SPSS for Windows (version 26.0; IBM Corp., Armonk, NY, USA). Bayesian multiple linear regression analysis was conducted using JASP version 0.17.1 (JASP Team). The statistical tests were two-tailed, and a P value $< 0.05/n$, calculated using the Bonferroni correction (where n refers to the number of multiple comparisons), was considered statistically significant. Under the assumption of a significant relationship, a P value < 0.05 was considered statistically significant.

3. Results

3.1. Parametric image analysis of the correlation between STAI scores and ^{11}C-DPA713-BP_{ND} values

Participant characteristics are summarized in Table.1 and box-plots of the value of CSF Aβ42/40 ratio and CSF p-tau 181 in Fig. 1

When we perform a correlation of Braak 1-3-^{11}C-DPA713-BP_{ND} with MMSE score, ADAS J-cog score, CSF Aβ42/40 ratio, CSF p-tau 181, and STAI-S and -T score trait, we found no significant association of DPA-713 SUVR with MMSE score ($r = -0.21$, $p = 0.39$), ADAS J-cog score ($r = -0.01$, $p = 0.98$), CSF Aβ42/40 ratio ($r = -0.15$, $p = 0.55$), CSF p-tau 181 ($r = 0.05$, $p = 0.85$) and STAI-S score ($r = 0.19$, $p = 0.44$) excepting STAI-T score ($r = 0.60$, $p = 0.006$).

In the whole-brain voxel-based parametric mapping, significant positive correlations were identified between STAI-T scores and regional

Table 1
Descriptive characteristics of patients with AD continuum.

Characteristic/Test	Patients with MCI	Patients with AD	Total patients
No.	5	14	19
Sex, M/F	3/2	6/8	9/10
Age, y, mean (SD)	80.0 (5.1)	77.7 (4.1)	78.3 (4.4)
Education, y, median (IQR)[a]	16 (12.5–16)	12 (10.5–12)	12 (12–16)
ApoE4(+)/(−)	2/3	8/6	10/9
MMSE, mean (SD)	26.6 (2.1)	20.7 (2.5)	22.3 (3.5)
ADAS-J-Cog score, mean (SD)	11.6 (7.2)	13.4 (4.8)	12.9 (5.4)
LM-1, median (IQR)	7.0 (4.0–14.5)	7.5 (4.0–10.3)	7 (4–10)
LM-2, median (IQR)[a]	0.0 (0.0–10.0)	0.0 (0.0–1.0)	0.0 (0.0–1.0)
CSF Aβ42/40 ratio values, median (IQR)[a]	0.035 (0.030–0.070)	0.052 (0.041–0.067)	0.050 (0.037–0.068)
CSF p-tau 181, median (IQR)[a]	48.7 (42.2–90.6)	46.7 (38.3–64.2)	48.7 (41.0–74.2)
STAI state score, mean (SD)	39.4 (12.8)	39.1 (5.1)	39.2 (7.4)
Low-to-intermediate (<45)	32.0 (9.5) (n = 3)	38.1 (4.8) (n = 12)	36.9 (6.1) (n = 15)
High (≥45)	50.5 (7.8) (n = 2)	45.0 (0.0) (n = 2)	47.8 (5.5) (n = 4)
STAI trait score, mean (SD)	45.8 (13.0)	44.1 (12.0)	44.5 (11.9)
Low-to-intermediate (<45)	34.0 (14.1) (n = 2)	35.4 (7.6) (n = 7)	35.1 (8.3) (n = 9)
High (≥45)	53.7 (2.1) (n = 3)	52.7 (9.0) (n = 7)	53.0 (7.4) (n = 10)
Braak 1-3-11C-DPA713-BP_{ND}, mean (SD)	0.12 (0.05)	0.14 (0.06)	0.13 (0.05)

Abbreviations: AD, Alzheimer's disease; MCI, Mild cognitive impairment; SD, standard deviation; IQR, Interquartile range; ApoE4, Apolipoprotein E4; MMSE, Mini-Mental State Examination; ADAS-J-Cog, Alzheimer's Disease Assessment Scale- Cognitive subscale (Japanese version); LM-1, Wechsler Logical Memory Scale I; LM-2, Wechsler Logical Memory Scale II; CSF, cerebrospinal fluid; STAI, State-Trait Anxiety Inventory.
[a] Non-normal distribution.

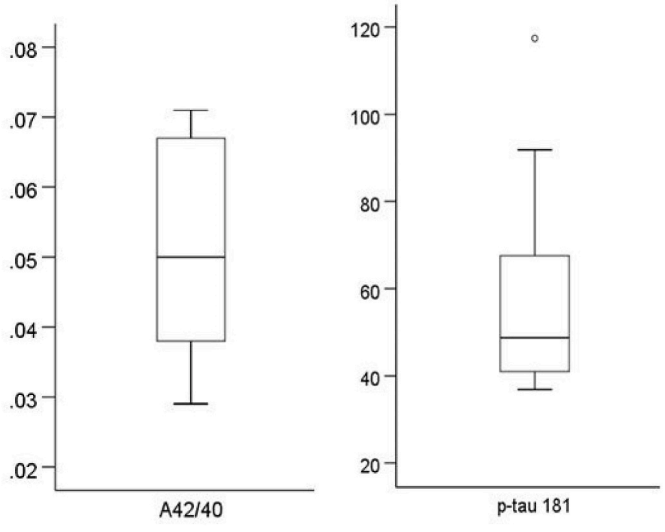

Fig. 1. Box-plots of the value of CSF Aβ42/40 ratio and CSF p-tau 181 (pg/mL).

^{11}C-DPA713-BP_{ND} values in clusters in the left inferior occipital area and bilateral centromedial amygdala (CMA) (Fig. 2, Table 2). No significant correlations were identified between STAI-S scores and regional ^{11}C-DPA713-BP_{ND} values. No significant correlations were identified between regional ^{11}C-DPA713-BP_{ND} values and CSF Aβ42/40 ratio and CSF p-tau 181 ($P < 0.001$, uncorrected).

Fig. 3 illustrates a scatterplot of the relationships between the STAI-T scores and ^{11}C-DPA713-BP_{ND} values in significant clusters. Pearson's correlation analyses revealed a significant relationship between STAI-T scores and ^{11}C-DPA713-BP_{ND} values in each cluster ($r = 0.84$, $P < 0.001$ for cluster #1; $r = 0.75$, $P < 0.001$ for cluster #2; and $r = 0.71$, $P = 0.001$ for cluster #3).

Mean VBM signals are 0.47 ± 0.07, 0.43 ± 0.06, 0.45 ± 0.07 for cluster#1, #2 and #3 respectively. We found no significant correlation between mean VBM signals and ^{11}C-DPA713-BP_{ND} values in these clusters. There was no significant correlation between the STAI-T scores and mean VBM signals in these clusters.

3.2. Stepwise multiple linear regression analysis

Table 3 presents the results of the stepwise multiple linear regression of STAI-T scores. The final model of this analysis included ^{11}C-DPA713-BP_{ND} values in cluster #1(occipital area) and #2 and #3 (amygdala), and Alzheimer's Disease Assessment Scale-Cognitive subscale (Japanese version) (ADAS-J-Cog) scores as predictors. Other variables such as age, sex, years of education, APOE4 positivity, Aβ42/40 ratio, and p-tau 181 concentration were excluded from the model. The STAI-T scores were significantly associated with ^{11}C-DPA713-BP_{ND} values in cluster #1 (occipital area) (standardized β [sβ] = 0.41, $P = 0.03$) and #2 and #3 (amygdala) (sβ = 0.48, $P = 0.01$) and ADAS-J-Cog scores (sβ = 0.34, $P = 0.01$).

3.3. Stepwise Bayesian regression analysis

Table 4 summarizes the final model, the list of models investigated, and their BF_{10} values in the stepwise Bayesian regression analysis of the STAI-T scores. The results of the stepwise Bayesian regression analysis were consistent with those of the stepwise linear multiple regression analysis (Table 3). A comparison of models using BF_{10}, with all brain measures and demographic variables as candidate predictors, suggested that the best model contained ^{11}C-DPA713-BP_{ND} values in clusters #1 (occipital area) and #2 and #3 (amygdala) and the ADAS-J-Cog score as a predictor of the STAI-T scores ($BF_{10} = 4.53 \times 10^3$; $R^2 = 0.83$).

3.4. ^{11}C-DPA713-BP_{ND} values in cluster #1- #3 in patients with AD continuum with low and high trait anxiety

Comparison of ^{11}C-DPA713-BP_{ND} values in clusters #1–3 using MANCOVA with the ADAS-J Cog score as a covariate revealed significantly higher ^{11}C-DPA713-BP_{ND} values in patients with AD continuum with high trait anxiety than in those with low trait anxiety. Under the assumption of a significant difference in ^{11}C-DPA713-BP_{ND} values, a follow-up analysis of covariance (ANCOVA) revealed that ^{11}C-DPA713-BP_{ND} values in each cluster were significantly higher in patients with high trait anxiety than in those with low trait anxiety (Table 5).

4. Discussion

This whole-brain voxel-based parametric mapping study investigated the correlation between anxiety severity and focal glial-mediated neuroinflammation, as indicated by STAI scores and ^{11}C-DPA713-BP_{ND}, respectively, in patients with AD continuum. It allows for the examination of the entire brain regions, providing a comprehensive view without restricting the analysis to predefined regions of interest. The results revealed a positive correlation between trait anxiety levels and ^{11}C-DPA713-BP_{ND} values in the bilateral CMA and the left inferior occipital area, and therefore we focused on these regions. Stepwise multiple linear regression analysis revealed that ^{11}C-DPA713-BP_{ND} values in the bilateral CMA and left occipital lobe, along with the ADAS-J Cog score, could predict STAI trait scores in patients with AD continuum. In contrast, Bayesian stepwise multiple regression analysis confirmed the

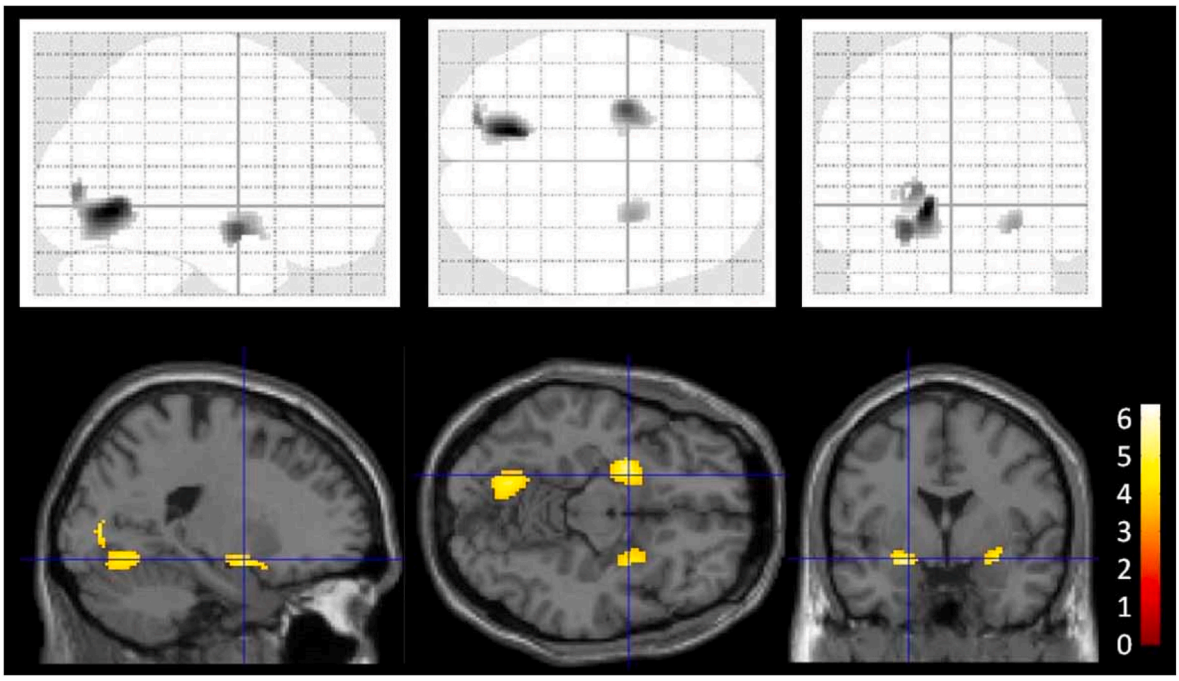

Fig. 2. Images of voxel-based maps exhibiting significant positive correlations between ^{11}C-DPA713-BP$_{ND}$ and the State-Trait Anxiety Inventory trait scores

Voxel-level at $P < 0.001$ (uncorrected) and a minimum cluster size of $k \geq 100$. Statistical parametric mapping projections are superimposed on representative sagittal (x = −20), transaxial (z = −12), and coronal (y = 0) magnetic resonance images.

Table 2

Clusters of regions with a significant correlation between the STAI trait score and regional^{11}C-DPA713-BP$_{ND}$ values.

Comparison	Brain region	MNI coordinates (x, y, z)[a]	t-value	Cluster size (voxels)	Mean ± SD of^{11}C-DPA713-BP$_{ND}$ value in the cluster
Negative correlation	none				
Positive correlation	Cluster #1: Left inferior occipital area			485	0.23 ± 0.06
	Lingual gyrus	−14, −64, −4	6.37		
	Cuneus	−18, −80, 6	4.86		
	Middle occipital gyrus	−26, −82, 4	4.18		
	Cluster #2: Left centromedial amygdala	−24, −2, −14	5.35	196	0.21 ± 0.08
	Cluster #3: Right centromedial amygdala	30, 0, −12	4.42	108	0.23 ± 0.08

Abbreviations: STAI, State-Trait Anxiety Inventory; BP$_{ND}$, binding potential; MNI: Montreal Neurological Institute; SD, standard deviation.

[a] x, y, and z reflect coordinates for peak voxel or other local maxima in MNI space.

validity of these values. This study found that patients with high trait anxiety had significantly higher ^{11}C-DPA713-BP$_{ND}$ values in each cluster than those with low trait anxiety. This study is the first to demonstrate a correlation between neuroinflammation and trait anxiety severity in brain regions associated with emotional processing, such as the amygdala and its associated regions, in patients with AD continuum.

In the whole-brain voxel-based parametric mapping, no significant correlations were identified between regional ^{11}C-DPA713-BP$_{ND}$ values and CSF Aβ42/40 ratio and CSF p-tau 181. While both amyloid beta and tau play important roles in the pathogenesis of Alzheimer's disease, tau pathology is regarded to be central to the neurodegenerative process and clinical manifestation of the disease (Nelson et al., 2012). Previous studies have reported inconsistent associations between tau and glial activation, considering the in vivo relationship between these pathological processes in AD (Dani et al., 2018; Parbo et al., 2018; Terada et al., 2019; Zou et al., 2020). In our study, the degree of glial activation was not correlated with the amount of tau pathology. Thus, tau toxicity is affected not only by the extent of tau pathology but also by other factors influencing tau-induced glial activation. The types of factors that influence tau-mediated glial stimulation remain unknown, and their identification is important for the development of therapeutic strategies to treat tauopathy.

In the previous longitudinal study (Yasuno et al., 2023), we found that TSPO-PET imaging of microglial activation is a stronger predictor of the progression of cognitive decline in AD. However, we found no significant relationship between ^{11}C-DPA713-BP$_{ND}$ and ADAS-J cog and MMSE score in this cross-sectional examination. Differences in results may occur because longitudinal studies provide insights into the temporal dynamics of phenomena, whereas cross-sectional studies do not capture changes over time. The effects of brain inflammation on

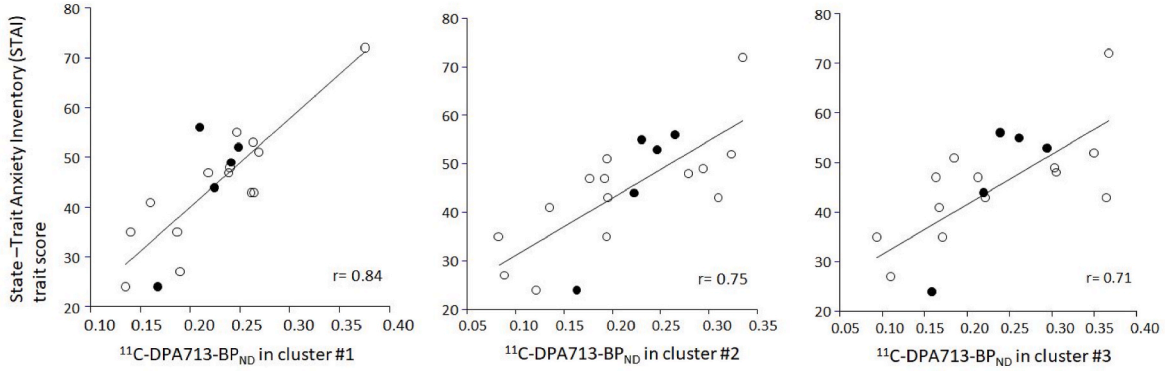

Fig. 3. Scatter plots of relationships between ^{11}C-DPA713-BP$_{ND}$ values in significant clusters from the voxel-based analysis and the State-Trait Anxiety Inventory trait scores (n = 19)
Filled circle: MCI, Unfilled circle: AD
r = 0.84, $P < 0.001$ for cluster #1; r = 0.75, $P < 0.001$ for cluster #2; and r = 0.71, $P = 0.001$ for cluster #3.

Table 3
Results of a stepwise multiple linear regression analysis predicting the STAI trait score.

Step	t	sβ	*P*	VIF	F	df	*P*	Adjusted R^2
Full Model					6.88	9, 9	0.004	0.75
Age	−0.32	−0.05	0.76	1.41				
Sex	0.53	0.08	0.61	1.76				
Education	0.49	0.06	0.64	1.23				
ADAS-J-Cog score	2.40	0.36	0.04	1.60				
ApoE4 positivity	0.89	0.15	0.40	2.05				
Aβ42/40	0.15	0.03	0.88	2.43				
p-tau 181	0.70	0.10	0.50	1.53				
^{11}C-DPA713-BP$_{ND}$ value in cluster #1 (occipital area)	1.99	0.43	0.08	3.35				
^{11}C-DPA713-BP$_{ND}$ value in cluster #2 & #3 (amygdala)	1.85	0.43	0.10	3.80				
Final model					10.9	3, 15	<0.001[a]	0.80
^{11}C-DPA713-BP$_{ND}$ value in cluster #1 (occipital area)	2.46	0.41	0.03	2.51				
^{11}C-DPA713-BP$_{ND}$ value in cluster #2 & #3 (amygdala)	2.97	0.48	0.01	2.35				
ADAS-J-Cog score	2.82	0.34	0.01	1.27				

Abbreviations: STAI, State-Trait Anxiety Inventory; sβ, Standardized β; VIF, Variance Inflation Factor; ADAS-J-Cog, 'Alzheimer's Disease Assessment Scale- Cognitive subscale (Japanese version); ApoE4, Apolipoprotein E4; BP$_{ND}$, binding potential.
[a] $P < 0.05$. R^2 = Multiple regression value squared.

cognitive decline may be based on long-term, gradual neurodegenerative processes and may not be reflected in cross-sectional studies. However, anxiety is likely to be an immediate consequence of inflammation in the brain, and cross-sectional studies may be more likely to detect its effects.

Previous studies identified the amygdala as a pivotal brain region for the expression of anxiety, signaling the existence of threats and salience information (Kujawa et al., 2016; Michely et al., 2020; Tovote et al., 2015). The amygdala, with its widespread connections to emotion-related cerebral regions, is considered an important neural hub for modulating anxiety-related behaviors (Asami et al., 2018). Anxiety may be triggered by information transmitted from the amygdala to other brain regions (Asami et al., 2018). Structural neuroimaging studies in both humans and animals that examined the association between anxiety severity and amygdala volume have consistently found a negative correlation between these variables (Foell et al., 2019; Pedraza et al., 2014; Yang et al., 2008; Zhao et al., 2013). Other neuroimaging studies have found that administering inflammatory stimuli affects brain regions involved in processing fear, anxiety, and emotions, such as the amygdala (Felger, 2018; Harrison, 2019). Notably, evidence of an association between inflammation and transdiagnostic symptoms such as anxiety has increasingly been demonstrated (Hou et al., 2017; Kennedy and Niedzwiedz, 2022; Milaneschi et al., 2021; van Eeden et al., 2021).

In the previous study, including a dual approach using stereological and proteomic techniques with the aim of assessing neuronal and glial involvement in the amygdala in AD, synaptic alterations, as well as the potential participation of glial cells in response to pathology have been identified as particularly relevant in amyloid pathology in AD (Gonzalez-Rodriguez et al., 2023). Progressively impaired amygdala intrinsic connectivity with other regions was also indicated in very early AD (Ortner et al., 2016). A central mechanism in the pathogenesis of anxiety disorders is associative learning or conditioning, which can lead to both conscious and unconscious aversive memories, and animal models and human studies have shown that the amygdala has a central role in the modulation of memory by emotion (de Quervain et al., 2017). Chronic exposure to stress causes anxiety, and a previous study showed that the inactivation of the amygdala in stressed rats prevents stress-induced anxiety (Tripathi et al., 2019b). In optogenetic approaches in behaving mice, activating the amygdala-medial prefrontal cortex (mPFC) projection increases anxiety-like behavior. It reduces social interaction, whereas inhibiting this pathway reduces anxiety-like behavior and increases social behavior. Such bidirectional modulation suggests that the pathway of the amygdala and its related region pathway is implicated in the regulation of the behavioral manifestations of anxiety and sociability (Felix-Ortiz et al., 2016).

The human amygdala comprises three major subregions: the CMA, basolateral amygdala (BLA), and superficial amygdala (SFA) (Amunts et al., 2005; Ball et al., 2007; Roy et al., 2009). Our voxel-based analysis revealed significant clusters in the CMA, which have been associated with depression and anxiety (Eckstein et al., 2017; Etkin et al., 2009). Abnormal dynamic functional connectivity of the CMA has been demonstrated in clinical depression (Qiu et al., 2018), while

Table 4
Results of the stepwise Bayesian multiple linear regression analysis predicting the STAI trait score.

Bayesian regression	β		95% Credible interval		
	Mean	SD	Lower	Upper	
The final model for predicting the STAI trait score					
ADAS-J-Cog score	0.69	0.26	0.16	1.23	
^{11}C-DPA713-BP$_{ND}$ value in cluster #1 (occipital area)	81.7	34.4	9.39	154.0	
^{11}C-DPA713-BP$_{ND}$ value in cluster #2 & #3 (amygdala)	68.4	23.9	18.3	118.6	
Models for predicting the STAI trait score[a]	P(M)	P(M| data)	BF_M	BF_{10}	R^2
ADAS-J-Cog score + ^{11}C-DPA713-BP$_{ND}$ value in cluster #1 (occipital area) + ^{11}C-DPA713-BP$_{ND}$ value in cluster #2 & #3 (amygdala)	0.002	0.064	35.0	4.53×10^3	0.83
ADAS-J-Cog score + ApoE4 positivity + ^{11}C-DPA713-BP$_{ND}$ value in cluster #1 (occipital area) + ^{11}C-DPA713-BP$_{ND}$ value in cluster #2 & #3 (amygdala)	0.002	0.032	16.9	2.26×10^3	0.85
ADAS-J-Cog score + ^{11}C-DPA713-BP$_{ND}$ value in cluster #2 & #3 (amygdala)	0.002	0.030	15.6	2.09×10^3	0.77
^{11}C-DPA713-BP$_{ND}$ value in cluster #1 (occipital area)	0.002	0.023	12.6	1.70×10^3	0.70
Sex + ^{11}C-DPA713-BP$_{ND}$ value in cluster #1 (occipital area)	0.002	0.022	12.0	1.62×10^3	0.76
Null model	0.002	1.42×10^{-5}	0.007	1.00	0

Abbreviations: STAI, State-Trait Anxiety Inventory; ADAS-J-Cog, Alzheimer's Disease Assessment Scale-Cognitive subscale (Japanese version); ApoE4, Apolipoprotein E4; BP$_{ND}$, binding potential.

[a] Models are presented as follows: higher Bayes Factor (BF_M) to lower. The table lists the five most likely models and the null model.

Table 5
^{11}C-DPA713-BP$_{ND}$ values in cluster #1–#3 in patients with AD continuum with low and high trait anxiety.

Region	Binding potential[a]					
	Low trait anxiety (n = 9)		High trait anxiety (n = 10)		Analysis of covariance	
	Mean	SD	Mean	SD	$F_{1, 16}$	*P*
^{11}C-DPA713-BP$_{ND}$ value in cluster #1 (occipital area)	0.19	0.05	0.26	0.05	6.80	0.02
^{11}C-DPA713-BP$_{ND}$ value in cluster #2 (left amygdala)	0.17	0.07	0.25	0.06	10.23	0.006
^{11}C-DPA713-BP$_{ND}$ value in cluster #3 (right amygdala)	0.19	0.08	0.27	0.07	6.86	0.02

Abbreviations: BP$_{ND}$, binding potential; AD, Alzheimer's disease; ADAS-J-Cog, Alzheimer's Disease Assessment Scale-Cognitive subscale (Japanese version); SD, standard deviation.

[a] Multivariate analysis of covariance with ADAS-J-Cog score as a covariate to test for group differences between patients with AD with low and high trait anxiety (Wilks' lambda = 0.53; F = 4.16, df = 3. 14, *P* = 0.03).

resting-state functional connectivity of the CMA may predict vulnerability to depression (Zhang et al., 2022). Moreover, the synaptic adhesion protein IgSF9b-in the CMA, which regulates anxiety-like behavior, is a target for anxiolytics (Babaev et al., 2018). The studies mentioned above support our findings of an association between inflammatory changes in the CMA and anxiety in patients with AD continuum. Previous neuroimaging studies have linked the CMA to behavioral response generation and attention allocation, the BLA to higher-order learning and sensory processes such as fear conditioning, and the SFA to social and emotional information processing (Bzdok et al., 2013; Goossens et al., 2009; LeDoux, 2003). Another study reported that functional connectivity of the CMA and BLA is associated with the control of emotional output and emotional information input, respectively (Li et al., 2012). In summary, anxiety in patients with AD continuum may mainly induced by the dysfunction of the control of emotional output related to behavioral responses and attention allocation, which the CMA subserves.

Several studies have reported on the role of the occipital lobe in anxiety. The amygdala projects directly into the ventral visual stream in the occipital lobe (Amaral et al., 2003; Amaral and Price, 1984) and modulates neuronal activity in these brain regions based on the affective stimulus properties (Phelps and LeDoux, 2005). A negative correlation was found between trait anxiety degree and gray matter volume in the middle occipital gyrus in healthy brain samples (Yin et al., 2016). Additionally, changes in network properties such as nodal degree and efficiency have been observed in the calcarine sulcus of individuals with social anxiety disorder (Yang et al., 2019). Thus, structural and functional changes in the occipital cortex may trigger or be a consequence of abnormal emotional information processing in patients with anxiety disorders. Previous studies have suggested that the occipital cortex is involved in uncertain cue processing (Zhang et al., 2016) and conscious processing (Yang et al., 2019). Individuals with anxiety tend to experience greater worry in uncertain situations (Zhang et al., 2016). Furthermore, the left hemisphere appears to play a more significant role in anxiety arousal than the right hemisphere (Heller et al., 1997). Inflammation-induced changes in the left occipital cortical activity may increase the risk of anxiety disorders by impairing uncertain cue processing.

In summary, the CMA–occipital lobe circuit controls emotional processing. The results of our TSPO-PET study revealed that disruption of this circuit by AD pathology-induced microglial- and astrocyte-mediated inflammation impairs emotional regulation and may contribute to anxiety. No significant correlations were identified between STAI-S scores and regional ^{11}C-DPA713-BP$_{ND}$ values. STAI-S focuses on the current emotional state, whereas STAI-T assesses a more enduring characteristic of an individual's personality related to anxiety. The CMA–occipital lobe circuit influences the control of emotional generation, and disruption of this network by AD pathology-induced inflammation may contribute to the expression of anxiety not temporarily or transitory but sustainably in everyday lives. Increasing evidence indicates that excessive inflammatory responses play a crucial role in the pathophysiology of psychiatric diseases, including depression and anxiety disorders (Park et al., 2018). Previous studies identified the amygdala as a pivotal brain region for the expression of anxiety, signaling the existence of threats and salience information (Kujawa et al., 2016; Michely et al., 2020; Tovote et al., 2015). Therefore, dysregulation of the amygdala and its projection areas may account for neuroinflammation-induced anxiety- and depressive-like behavior. Our results are consistent with this notion and show that this theory is applicable to anxiety in AD. Our findings support the hypothesis that inflammation reduction or anti-inflammatory signaling enhancement, achieved by reducing damage to the amygdala and its associated regions, can be effective anxiety treatment strategies.

In preclinical studies, some phenyl benzoxazole or piperazine derivatives are shown to be effective as a potent acetylcholinesterase inhibitor with antioxidant properties (Srivastava et al., 2019; Tripathi et al., 2019a). Mitochondrial dysfunction plays a vital role in the pathogenesis of AD, and antioxidants like coenzyme Q and glutathione can reduce the production of mitochondrial reactive oxygen species and oxidative stress and also decrease the process of inflammation (Rai et al., 2020). As another immunologic intervention, mild endoplasmic reticulum stress (MERS) preconditioning is shown to be able to alleviate neuroinflammation and cognitive impairment, thereby suggesting that

moderate level of ER stress can act as a new therapeutic possibility to delay the progression of neurodegenerative diseases (Rai et al., 2018; Wang et al., 2017). These immunologic interventions targeting neuroinflammation pathways could be explored in preclinical models to evaluate their potential efficacy in reducing anxiety symptoms in AD.

This study has some limitations. First, the findings were based on modest sample size; nevertheless, the agreement between different statistical models mitigated sample bias. The study results need to be validated in larger clinical cohorts to establish their reproducibility and generalizability. Second, the study included only participants with MCI and mild-to-moderate AD, and TSPO binding was poorly observed in the neocortical regions at this disease stage. Therefore, the correlation between trait anxiety and TSPO binding in the amygdala and occipital lobe suggests that it is a sensitive, albeit specific marker of anxiety symptoms. Future studies involving patients with more severe AD are necessary to clarify the involvement of neuroinflammation in other neocortical regions. Third, there are no matched healthy control subjects enrolled in the study as a comparison, as the focus of this study is on understanding the effect of pathological neuroinflammation on anxiety within the AD continuum. A future study is necessary to determine whether the same correlation exists between trait anxiety and inflammation in healthy subjects without AD pathology. Fourth, anxiety levels were evaluated using the STAI in this study. Some patients with relatively late disease stages may not answer these questions correctly. In regards to the issue of the ability to consent to this study, only MCI and mild-to-moderate AD were included. In the examination of the anxiety of patients with late disease stage, different evaluation methods of anxiety are necessary. Fifth, the direction of causality between anxiety and TSPO binding could not be determined in this study. We speculate that these factors influence each other. Therefore, future longitudinal immunologic intervention studies that assess changes in anxiety and TSPO binding could clarify the strength of this relationship.

5. Conclusions

Our voxel-based analysis revealed a positive correlation between trait anxiety levels and ^{11}C-DPA713-BP$_{ND}$ values in the CMA and the left inferior occipital area in patients with AD continuum. The degree of trait anxiety in patients with AD continuum as strongly predicted by ^{11}C-DPA713-BP$_{ND}$ in these regions. Additionally, patients with AD continuum and high trait anxiety exhibited increased ^{11}C-DPA713-BP$_{ND}$ in these regions. These findings suggest the involvement of glial-mediated neuroinflammation in the amygdala and its associated regions in the development of trait anxiety in patients with AD continuum. Immunologic interventions for anxiety may be an alternative treatment for dementia. In future studies, non-invasive neuroimaging techniques, combined with biochemical assays or genetic analyses, are to be employed to elucidate further the molecular mechanisms linking glial-mediated neuroinflammation to anxiety severity in patients with AD.

Funding

This research was supported by the Japan Society for the Promotion of Science (KAKENHI [grant number: 22K07610]), the National Center for Geriatrics and Gerontology (Research Funding for Longevity Sciences [grant numbers: 22-5, 22–23] to FY), and the Japan Agency for Medical Research and Development (AMED [grant numbers: JP23dk0207059, JP23dm0207073] to TI).

Data statement

The data that support the findings of this study are available from the corresponding author upon reasonable request.

CRediT authorship contribution statement

Fumihiko Yasuno: Writing – original draft, Resources, Methodology, Investigation, Funding acquisition, Formal analysis, Conceptualization. **Yasuyuki Kimura:** Writing – review & editing, Validation, Resources, Methodology, Investigation, Formal analysis, Data curation. **Aya Ogata:** Writing – review & editing, Resources, Investigation. **Hiroshi Ikenuma:** Writing – review & editing, Resources, Investigation. **Junichiro Abe:** Writing – review & editing, Resources, Investigation. **Hiroyuki Minami:** Writing – review & editing, Resources, Investigation. **Takashi Nihashi:** Writing – review & editing, Resources, Investigation. **Kastunori Yokoi:** Writing – review & editing, Resources, Investigation. **Saori Hattori:** Writing – review & editing, Resources, Investigation. **Nobuyoshi Shimoda:** Writing – review & editing, Resources, Investigation. **Atsushi Watanabe:** Writing – review & editing, Resources, Investigation. **Kensaku Kasuga:** Writing – review & editing, Resources, Investigation. **Takeshi Ikeuchi:** Writing – review & editing, Resources, Investigation, Funding acquisition. **Akinori Takeda:** Writing – review & editing. **Takashi Sakurai:** Writing – review & editing. **Kengo Ito:** Writing – review & editing. **Takashi Kato:** Writing – review & editing, Project administration.

Declaration of competing interest

The authors declare that they have no known competing financial interests or personal relationships that could have appeared to influence the work reported in this paper.

Data availability

Data will be made available on request.

Acknowledgments

We wish to thank the National Center for Geriatrics and Gerontology Biobank for their assistance with the quality control of the clinical data, Yoko Arai for her exceptional patient care, and Hiroshi Morisihita and team (radiology technicians) for their invaluable support with the PET scans.

References

Amaral, D.G., Behniea, H., Kelly, J.L., 2003. Topographic organization of projections from the amygdala to the visual cortex in the macaque monkey. Neuroscience 118, 1099–1120. https://doi.org/10.1016/s0306-4522(02)01001-1.

Amaral, D.G., Price, J.L., 1984. Amygdalo-cortical projections in the monkey (Macaca fascicularis). J. Comp. Neurol. 230, 465–496. https://doi.org/10.1002/cne.902300402.

Amunts, K., Kedo, O., Kindler, M., Pieperhoff, P., Mohlberg, H., Shah, N.J., Habel, U., Schneider, F., Zilles, K., 2005. Cytoarchitectonic mapping of the human amygdala, hippocampal region and entorhinal cortex: intersubject variability and probability maps. Anat. Embryol. 210, 343–352. https://doi.org/10.1007/s00429-005-0025-5.

Asami, T., Nakamura, R., Takaishi, M., Yoshida, H., Yoshimi, A., Whitford, T.J., Hirayasu, Y., 2018. Smaller volumes in the lateral and basal nuclei of the amygdala in patients with panic disorder. PLoS One 13, e0207163. https://doi.org/10.1371/journal.pone.0207163.

Ashburner, J., Friston, K.J., 2000. Voxel-based morphometry–the methods. Neuroimage 11, 805–821. https://doi:10.1006/nimg.2000.0582.

Ashburner, J., Friston, K.J., 2005. Unified segmentation. Neuroimage 26, 839–851. https://10.1016/j.neuroimage.2005.02.018.

Babaev, O., Cruces-Solis, H., Piletti Chatain, C., Hammer, M., Wenger, S., Ali, H., Karalis, N., de Hoz, L., Schlüter, O.M., Yanagawa, Y., Ehrenreich, H., Taschenberger, H., Brose, N., Krueger-Burg, D., 2018. IgSF9b regulates anxiety behaviors through effects on centromedial amygdala inhibitory synapses. Nat. Commun. 9, 5400. https://doi.org/10.1038/s41467-018-07762-1.

Ball, T., Rahm, B., Eickhoff, S.B., Schulze-Bonhage, A., Speck, O., Mutschler, I., 2007. Response properties of human amygdala subregions: evidence based on functional MRI combined with probabilistic anatomical maps. PLoS One 2, e307. https://doi.org/10.1371/journal.pone.0000307.

Banati, R.B., Egensperger, R., Maassen, A., Hager, G., Kreutzberg, G.W., Graeber, M.B., 2004. Mitochondria in activated microglia in vitro. J. Neurocytol. 33, 535–541. https://doi.org/10.1007/s11068-004-0515-7.

Bogavac, I., Jeličić, L., Đorđević, J., Veselinović, I., Marisavljević, M., Subotić, M., 2023. Comparing anxiety levels during the COVID-19 pandemic among mothers of children with and without neurodevelopmental disorders. Children 10, 1292. https://doi.org/10.3390/children10081292.

Braak, H., Braak, E., 1991. Neuropathological stageing of Alzheimer-related changes. Acta Neuropathol. 82, 239–259. https://doi.org/10.1007/bf00308809.

Bzdok, D., Laird, A.R., Zilles, K., Fox, P.T., Eickhoff, S.B., 2013. An investigation of the structural, connectional, and functional subspecialization in the human amygdala. Hum Brain Mapp 34, 3247–3266. https://doi.org/10.1002/hbm.22138.

Calsolaro, V., Edison, P., 2016. Neuroinflammation in Alzheimer's disease: current evidence and future directions. Alzheimers Dement 12, 719–732. https://doi.org/10.1016/j.jalz.2016.02.010.

Dani, M., Wood, M., Mizoguchi, R., Fan, Z., Walker, Z., Morgan, R., Hinz, R., Biju, M., Kuruvilla, T., Brooks, D.J., Edison, P., 2018. Microglial activation correlates in vivo with both tau and amyloid in Alzheimer's disease. Brain 141, 2740–2754. https://10.1093/brain/awy188.

de Quervain, D., Schwabe, L., Roozendaal, B., 2017. Stress, glucocorticoids and memory: implications for treating fear-related disorders. Nat. Rev. Neurosci. 18, 7–19. https://10.1038/nrn.2016.155.

Demnitz-King, H., Saba, L., Lau, Y., Munns, L., Zabihi, S., Schlosser, M., Del-Pino-Casado, R., Orgeta, V., Marchant, N.L., 2023. Association between anxiety symptoms and Alzheimer's disease biomarkers in cognitively healthy adults: a systematic review and meta-analysis. J. Psychosom. Res. 166, 111159 https://doi.org/10.1016/j.jpsychores.2023.111159.

Eckstein, M., Markett, S., Kendrick, K.M., Ditzen, B., Liu, F., Hurlemann, R., Becker, B., 2017. Oxytocin differentially alters resting state functional connectivity between amygdala subregions and emotional control networks: inverse correlation with depressive traits. Neuroimage 149, 458–467. https://doi.org/10.1016/j.neuroimage.2017.01.078.

Etkin, A., Prater, K.E., Schatzberg, A.F., Menon, V., Greicius, M.D., 2009. Disrupted amygdalar subregion functional connectivity and evidence of a compensatory network in generalized anxiety disorder. Arch. Gen. Psychiatr. 66, 1361–1372. https://doi.org/10.1001/archgenpsychiatry.2009.104.

Felger, J.C., 2018. Imaging the role of inflammation in mood and anxiety-related disorders. Curr. Neuropharmacol. 16, 533–558. https://doi.org/10.2174/1570159x15666171123201142.

Felix-Ortiz, A.C., Burgos-Robles, A., Bhagat, N.D., Leppla, C.A., Tye, K.M., 2016. Bidirectional modulation of anxiety-related and social behaviors by amygdala projections to the medial prefrontal cortex. Neuroscience 321, 197–209. https://10.1016/j.neuroscience.2015.07.041.

Foell, J., Palumbo, I.M., Yancey, J.R., Vizueta, N., Demirakca, T., Patrick, C.J., 2019. Biobehavioral threat sensitivity and amygdala volume: a twin neuroimaging study. Neuroimage 186, 14–21. https://doi.org/10.1016/j.neuroimage.2018.10.065.

Fujita, M., Kobayashi, M., Ikawa, M., Gunn, R.N., Rabiner, E.A., Owen, D.R., Zoghbi, S.S., Haskali, M.B., Telu, S., Pike, V.W., Innis, R.B., 2017. Comparison of four (11)C-labeled PET ligands to quantify translocator protein 18 kDa (TSPO) in human brain: (R)-PK11195, PBR28, DPA-713, and ER176-based on recent publications that measured specific-to-non-displaceable ratios. EJNMMI Res. 7, 84. https://doi.org/10.1186/s13550-017-0334-8.

Fulton, S., Décarie-Spain, L., Fioramonti, X., Guiard, B., Nakajima, S., 2022. The menace of obesity to depression and anxiety prevalence. Trends Endocrinol. Metabol. 33, 18–35. https://doi.org/10.1016/j.tem.2021.10.005.

Gonzalez-Rodriguez, M., Villar-Conde, S., Astillero-Lopez, V., Villanueva-Anguita, P., Ubeda-Banon, I., Flores-Cuadrado, A., Martinez-Marcos, A., Saiz-Sanchez, D., 2023. Human amygdala involvement in Alzheimer's disease revealed by stereological and dia-PASEF analysis. Brain Pathol. 33, e13180. https://10.1111/bpa.13180.

Goossens, L., Kukolja, J., Onur, O.A., Fink, G.R., Maier, W., Griez, E., Schruers, K., Hurlemann, R., 2009. Selective processing of social stimuli in the superficial amygdala. Hum Brain Mapp 30, 3332–3338. https://doi.org/10.1002/hbm.20755.

Harrison, N.A., 2019. Disentangling the effects of peripheral inflammatory markers on brain functional connectivity. Biol. Psychiatr. 86, 84–86. https://doi.org/10.1016/j.biopsych.2019.05.013.

Hayasaka, S., Nichols, T.E., 2004. Combining voxel intensity and cluster extent with permutation test framework. Neuroimage 23, 54–63. https://doi.org/10.1016/j.neuroimage.2004.04.035.

Heller, W., Nitschke, J.B., Etienne, M.A., Miller, G.A., 1997. Patterns of regional brain activity differentiate types of anxiety. J. Abnorm. Psychol. 106, 376–385. https://doi.org/10.1037//0021-843x.106.3.376.

Heneka, M.T., Carson, M.J., El Khoury, J., Landreth, G.E., Brosseron, F., Feinstein, D.L., Jacobs, A.H., Wyss-Coray, T., Vitorica, J., Ransohoff, R.M., Herrup, K., Frautschy, S. A., Finsen, B., Brown, G.C., Verkhratsky, A., Yamanaka, K., Koistinaho, J., Latz, E., Halle, A., Petzold, G.C., Town, T., Morgan, D., Shinohara, M.L., Perry, V.H., Holmes, C., Bazan, N.G., Brooks, D.J., Hunot, S., Joseph, B., Deigendesch, N., Garaschuk, O., Boddeke, E., Dinarello, C.A., Breitner, J.C., Cole, G.M., Golenbock, D. T., Kummer, M.P., 2015. Neuroinflammation in Alzheimer's disease. Lancet Neurol. 14, 388–405. https://doi.org/10.1016/s1474-4422(15)70016-5.

Hixson, J.E., Vernier, D.T., 1990. Restriction isotyping of human apolipoprotein E by gene amplification and cleavage with HhaI. J. Lipid Res. 31, 545–548. https://doi.org/10.1016/S0022-2275(20)43176-1.

Hou, R., Garner, M., Holmes, C., Osmond, C., Teeling, J., Lau, L., Baldwin, D.S., 2017. Peripheral inflammatory cytokines and immune balance in generalised anxiety disorder: case-controlled study. Brain Behav. Immun. 62, 212–218. https://doi.org/10.1016/j.bbi.2017.01.021.

Kass, R.E., Raftery, A.E., 1995. Bayes factors. J. Am. Stat. Assoc. 90, 773–795. https://doi.org/10.1080/01621459.1995.10476572.

Kasuga, K., Kikuchi, M., Tsukie, T., Suzuki, K., Ihara, R., Iwata, A., Hara, N., Miyashita, A., Kuwano, R., Iwatsubo, T., Ikeuchi, T., 2022. Different AT(N) profiles and clinical progression classified by two different N markers using total tau and neurofilament light chain in cerebrospinal fluid. BMJ Neurol. Open 4, e000321. https://doi.org/10.1136/bmjno-2022-000321.

Kasuga, K., Tsukie, T., Kikuchi, M., Tokutake, T., Washiyama, K., Shimizu, S., Yoshizawa, H., Kuroha, Y., Yajima, R., Mori, H., Arakawa, Y., Onda, K., Miyashita, A., Onodera, O., Iwatsubo, T., Ikeuchi, T., Japanese Alzheimer's Disease Neuroimaging Initiative, 2023. The clinical application of optimized AT(N) classification in Alzheimer's clinical syndrome (ACS) and non-ACS conditions. Neurobiol. Aging 127, 23–32. https://doi.org/10.1016/j.neurobiolaging.2023.03.007.

Kennedy, E., Niedzwiedz, C.L., 2022. The association of anxiety and stress-related disorders with C-reactive protein (CRP) within UK Biobank. Brain Behav. Immun. Health 19, 100410. https://doi.org/10.1016/j.bbih.2021.100410.

Kujawa, A., Wu, M., Klumpp, H., Pine, D.S., Swain, J.E., Fitzgerald, K.D., Monk, C.S., Phan, K.L., 2016. Altered development of amygdala-anterior cingulate cortex connectivity in anxious youth and young adults. Biol. Psychiatry Cogn. Neurosci. Neuroimaging. 1, 345–352. https://doi.org/10.1016/j.bpsc.2016.01.006.

Li, Y., Qin, W., Jiang, T., Zhang, Y., Yu, C., 2012. Sex-dependent correlations between the personality dimension of harm avoidance and the resting-state functional connectivity of amygdala subregions. PLoS One 7, e35925. https://doi.org/10.1371/journal.pone.0035925.

Liu, H.Y., Yue, J., Hu, L.N., Cheng, L.F., Wang, X.S., Wang, X.J., Feng, B., 2018. Chronic minocycline treatment reduces the anxiety-like behaviors induced by repeated restraint stress through modulating neuroinflammation. Brain Res. Bull. 143, 19–26. https://doi.org/10.1016/j.brainresbull.2018.08.015.

Malpetti, M., Kievit, R.A., Passamonti, L., Jones, P.S., Tsvetanov, K.A., Rittman, T., Mak, E., Nicastro, N., Bevan-Jones, W.R., Su, L., Hong, Y.T., Fryer, T.D., Aigbirhio, F. I., O'Brien, J.T., Rowe, J.B., 2020. Microglial activation and tau burden predict cognitive decline in Alzheimer's disease. Brain 143, 1588–1602. https://doi.org/10.1093/brain/awaa088.

McKhann, G.M., Knopman, D.S., Chertkow, H., Hyman, B.T., Jack Jr., C.R., Kawas, C.H., Klunk, W.E., Koroshetz, W.J., Manly, J.J., Mayeux, R., Mohs, R.C., Morris, J.C., Rossor, M.N., Scheltens, P., Carrillo, M.C., Thies, B., Weintraub, S., Phelps, C.H., 2011. The diagnosis of dementia due to Alzheimer's disease: recommendations from the National Institute on Aging-Alzheimer's Association workgroups on diagnostic guidelines for Alzheimer's disease. Alzheimers Dement 7, 263–269. https://doi.org/10.1016/j.jalz.2011.03.005.

Mega, M.S., Cummings, J.L., Fiorello, T., Gornbein, J., 1996. The spectrum of behavioral changes in Alzheimer's disease. Neurology 46, 130–135. https://doi.org/10.1212/wnl.46.1.130.

Mhatre, S.D., Tsai, C.A., Rubin, A.J., James, M.L., Andreasson, K.I., 2015. Microglial malfunction: the third rail in the development of Alzheimer's disease. Trends Neurosci. 38, 621–636. https://doi.org/10.1016/j.tins.2015.08.006.

Michely, J., Rigoli, F., Rutledge, R.B., Hauser, T.U., Dolan, R.J., 2020. Distinct processing of aversive experience in amygdala subregions. Biol. Psychiatry Cogn. Neurosci. Neuroimaging. 5, 291–300. https://doi.org/10.1016/j.bpsc.2019.07.008.

Milaneschi, Y., Kappelmann, N., Ye, Z., Lamers, F., Moser, S., Jones, P.B., Burgess, S., Penninx, B., Khandaker, G.M., 2021. Association of inflammation with depression and anxiety: evidence for symptom-specificity and potential causality from UK Biobank and NESDA cohorts. Mol. Psychiatr. 26, 7393–7402. https://doi.org/10.1038/s41380-021-01188-w.

Mintzer, J.E., Brawman-Mintzer, O., 1996. Agitation as a possible expression of generalized anxiety disorder in demented elderly patients: toward a treatment approach. J. Clin. Psychiatry 57, 55–63.

Nelson, P.T., Alafuzoff, I., Bigio, E.H., Bouras, C., Braak, H., Cairns, N.J., Castellani, R.J., Crain, B.J., Davies, P., Del Tredici, K., Duyckaerts, C., Frosch, M.P., Haroutunian, V., Hof, P.R., Hulette, C.M., Hyman, B.T., Iwatsubo, T., Jellinger, K.A., Jicha, G.A., Kövari, E., Kukull, W.A., Leverenz, J.B., Love, S., Mackenzie, I.R., Mann, D.M., Masliah, E., McKee, A.C., Montine, T.J., Morris, J.C., Schneider, J.A., Sonnen, J.A., Thal, D.R., Trojanowski, J.Q., Troncoso, J.C., Wisniewski, T., Woltjer, R.L., Beach, T. G., 2012. Correlation of Alzheimer disease neuropathologic changes with cognitive status: a review of the literature. J. Neuropathol. Exp. Neurol. 71, 362–381. https://10.1097/NEN.0b013e31825018f7.

Ortner, M., Pasquini, L., Barat, M., Alexopoulos, P., Grimmer, T., Förster, S., Diehl-Schmid, J., Kurz, A., Förstl, H., Zimmer, C., Wohlschläger, A., Sorg, C., Peters, H., 2016. Progressively disrupted intrinsic functional connectivity of basolateral amygdala in very early Alzheimer's disease. Front. Neurol. 7, 132. https://10.3389/fneur.2016.00132.

Owen, D.R., Gunn, R.N., Rabiner, E.A., Bennacef, I., Fujita, M., Kreisl, W.C., Innis, R.B., Pike, V.W., Reynolds, R., Matthews, P.M., Parker, C.A., 2011. Mixed-affinity binding in humans with 18-kDa translocator protein ligands. J. Nucl. Med. 52, 24–32. https://doi.org/10.2967/jnumed.110.079459.

Parbo, P., Ismail, R., Sommerauer, M., Stokholm, M.G., Hansen, A.K., Hansen, K.V., Amidi, A., Schaldemose, J.L., Gottrup, H., Brændgaard, H., Eskildsen, S.F., Borghammer, P., Hinz, R., Aanerud, J., Brooks, D.J., 2018. Does inflammation precede tau aggregation in early Alzheimer's disease? A PET study. Neurobiol. Dis. 117, 211–216. https://10.1016/j.nbd.2018.06.004.

Park, C., Brietzke, E., Rosenblat, J.D., Musial, N., Zuckerman, H., Ragguett, R.M., Pan, Z., Rong, C., Fus, D., McIntyre, R.S., 2018. Probiotics for the treatment of depressive symptoms: an anti-inflammatory mechanism? Brain Behav. Immun. 73, 115–124. https://10.1016/j.bbi.2018.07.006.

Pedraza, C., Sánchez-López, J., Castilla-Ortega, E., Rosell-Valle, C., Zambrana-Infantes, E., García-Fernández, M., Rodriguez de Fonseca, F., Chun, J., Santín, L.J., Estivill-Torrús, G., 2014. Fear extinction and acute stress reactivity reveal a role of

LPA(1) receptor in regulating emotional-like behaviors. Brain Struct. Funct. 219, 1659–1672. https://doi.org/10.1007/s00429-013-0592-9.
Phelps, E.A., LeDoux, J.E., 2005. Contributions of the amygdala to emotion processing: from animal models to human behavior. Neuron 48, 175–187. https://doi.org/10.1016/j.neuron.2005.09.025.
Qiu, L., Xia, M., Cheng, B., Yuan, L., Kuang, W., Bi, F., Ai, H., Gu, Z., Lui, S., Huang, X., He, Y., Gong, Q., 2018. Abnormal dynamic functional connectivity of amygdalar subregions in untreated patients with first-episode major depressive disorder. J. Psychiatry Neurosci. 43, 262–272. https://doi.org/10.1503/jpn.170112.
Rai, S.N., Singh, C., Singh, A., Singh, M.P., Singh, B.K., 2020. Mitochondrial dysfunction: a potential therapeutic target to treat Alzheimer's disease. Mol. Neurobiol. 57, 3075–3088. https://10.1007/s12035-020-01945-y.
Rai, S.N., Zahra, W., Birla, H., Singh, S.S., Singh, S.P., 2018. Commentary: mild endoplasmic reticulum stress ameliorates lpopolysaccharide-induced neuroinflammation and cognitive impairment via regulation of microglial polarization. Front. Aging Neurosci. 10, 192. https://10.1007/s12035-020-01945-y.
Roy, A.K., Shehzad, Z., Margulies, D.S., Kelly, A.M., Uddin, L.Q., Gotimer, K., Biswal, B. B., Castellanos, F.X., Milham, M.P., 2009. Functional connectivity of the human amygdala using resting state fMRI. Neuroimage 45, 614–626. https://doi.org/10.1016/j.neuroimage.2008.11.030.
Spielberger, C.D., Gorsuch, R.L., Lushene, R., Vagg, P.R., Jacobs, G.A., 1983. Manual for the State-Trait Anxiety Inventory STAI. Consulting Psychologists Press, Palo Alto, CA.
Srivastava, P., Tripathi, P.N., Sharma, P., Rai, S.N., Singh, S.P., Srivastava, R.K., Shankar, S., Shrivastava, S.K., 2019. Design and development of some phenyl benzoxazole derivatives as a potent acetylcholinesterase inhibitor with antioxidant property to enhance learning and memory. Eur. J. Med. Chem. 163, 116–135. https://10.1016/j.ejmech.2018.11.049.
Terada, T., Yokokura, M., Obi, T., Bunai, T., Yoshikawa, E., Ando, I., Shimada, H., Suhara, T., Higuchi, M., Ouchi, Y., 2019. In vivo direct relation of tau pathology with neuroinflammation in early Alzheimer's disease. J. Neurol. 266, 2186–2196. https://10.1007/s00415-019-09400-2.
Teri, L., Ferretti, L.E., Gibbons, L.E., Logsdon, R.G., McCurry, S.M., Kukull, W.A., McCormick, W.C., Bowen, J.D., Larson, E.B., 1999. Anxiety of Alzheimer's disease: prevalence, and comorbidity. J. Gerontol. A. Biol. Sci. Med. Sci. 54, M348–M352. https://doi.org/10.1093/gerona/54.7.m348.
Tovote, P., Fadok, J.P., Lüthi, A., 2015. Neuronal circuits for fear and anxiety. Nat. Rev. Neurosci. 16, 317–331. https://doi.org/10.1038/nrn3945.
Tripathi, P.N., Srivastava, P., Sharma, P., Tripathi, M.K., Seth, A., Tripathi, A., Rai, S.N., Singh, S.P., Shrivastava, S.K., 2019a. Biphenyl-3-oxo-1,2,4-triazine linked piperazine derivatives as potential cholinesterase inhibitors with anti-oxidant property to improve the learning and memory. Bioorg. Chem. 85, 82–96. https://10.1016/j.bioorg.2018.12.017.
Tripathi, S.J., Chakraborty, S., Srikumar, B.N., Raju, T.R., Shankaranarayana Rao, B.S., 2019b. Basolateral amygdalar inactivation blocks chronic stress-induced lamina-specific reduction in prefrontal cortex volume and associated anxiety-like behavior. Prog. Neuro-Psychopharmacol. Biol. Psychiatry 88, 194–207. https://10.1016/j.pnpbp.2018.07.016.
Tzourio-Mazoyer, N., Landeau, B., Papathanassiou, D., Crivello, F., Etard, O., Delcroix, N., Mazoyer, B., Joliot, M., 2002. Automated anatomical labeling of activations in SPM using a macroscopic anatomical parcellation of the MNI MRI single-subject brain. Neuroimage 15, 273–289. https://doi.org/10.1006/nimg.2001.0978.
van Eeden, W.A., El Filali, E., van Hemert, A.M., Carlier, I.V.E., Penninx, B., Lamers, F., Schoevers, R., Giltay, E.J., 2021. Basal and LPS-stimulated inflammatory markers and the course of anxiety symptoms. Brain Behav. Immun. 98, 378–387. https://doi.org/10.1016/j.bbi.2021.09.001.
Wang, Y.L., Han, Q.Q., Gong, W.Q., Pan, D.H., Wang, L.Z., Hu, W., Yang, M., Li, B., Yu, J., Liu, Q., 2018. Microglial activation mediates chronic mild stress-induced depressive- and anxiety-like behavior in adult rats. J. Neuroinflammation 15, 21. https://doi.org/10.1186/s12974-018-1054-3.
Wang, Y.W., Zhou, Q., Zhang, X., Qian, Q.Q., Xu, J.W., Ni, P.F., Qian, Y.N., 2017. Mild endoplasmic reticulum stress ameliorates lipopolysaccharide-induced neuroinflammation and cognitive impairment via regulation of microglial polarization. J. Neuroinflammation 14, 233. https://10.1186/s12974-017-1002-7.
Yang, R.J., Mozhui, K., Karlsson, R.M., Cameron, H.A., Williams, R.W., Holmes, A., 2008. Variation in mouse basolateral amygdala volume is associated with differences in stress reactivity and fear learning. Neuropsychopharmacology 33, 2595–2604. https://doi.org/10.1038/sj.npp.1301665.
Yang, X., Liu, J., Meng, Y., Xia, M., Cui, Z., Wu, X., Hu, X., Zhang, W., Gong, G., Gong, Q., Sweeney, J.A., He, Y., 2019. Network analysis reveals disrupted functional brain circuitry in drug-naive social anxiety disorder. Neuroimage 190, 213–223. https://doi.org/10.1016/j.neuroimage.2017.12.011.
Yasuno, F., Kimura, Y., Ogata, A., Ikenuma, H., Abe, J., Minami, H., Nihashi, T., Yokoi, K., Hattori, S., Shimoda, N., Ichise, M., Sakurai, T., Ito, K., Kato, T., 2022. Kinetic modeling and non-invasive approach for translocator protein quantification with (11)C-DPA-713. Nucl. Med. Biol. 108–109, 76–84. https://doi.org/10.1016/j.nucmedbio.2022.02.005.
Yasuno, F., Kimura, Y., Ogata, A., Ikenuma, H., Abe, J., Minami, H., Nihashi, T., Yokoi, K., Hattori, S., Shimoda, N., Watanabe, A., Kasuga, K., Ikeuchi, T., Takeda, A., Sakurai, T., Ito, K., Kato, T., 2023. Neuroimaging biomarkers of glial activation for predicting the annual cognitive function decline in patients with Alzheimer's disease. Brain Behav. Immun. 114, 214–220. https://doi.org/10.1016/j.bbi.2023.08.027.
Yin, P., Zhang, M., Hou, X., Tan, Y., Fu, Y., Qiu, J., 2016. The brain structure and spontaneous activity baseline of the behavioral bias in trait anxiety. Behav. Brain Res. 312, 355–361. https://doi.org/10.1016/j.bbr.2016.06.036.
Zhang, M., Ma, C., Luo, Y., Li, J., Li, Q., Liu, Y., Ding, C., Qiu, J., 2016. Neural basis of uncertain cue processing in trait anxiety. Sci. Rep. 6, 21298 https://doi.org/10.1038/srep21298.
Zhang, S., Cui, J., Zhang, Z., Wang, Y., Liu, R., Chen, X., Feng, Y., Zhou, J., Zhou, Y., Wang, G., 2022. Functional connectivity of amygdala subregions predicts vulnerability to depression following the COVID-19 pandemic. J. Affect. Disord. 297, 421–429. https://doi.org/10.1016/j.jad.2021.09.107.
Zhao, K., Yan, W.J., Chen, Y.H., Zuo, X.N., Fu, X., 2013. Amygdala volume predicts inter-individual differences in fearful face recognition. PLoS One 8, e74096. https://doi.org/10.1371/journal.pone.0074096.
Zhao, Q.F., Tan, L., Wang, H.F., Jiang, T., Tan, M.S., Tan, L., Xu, W., Li, J.Q., Wang, J., Lai, T.J., Yu, J.T., 2016. The prevalence of neuropsychiatric symptoms in Alzheimer's disease: systematic review and meta-analysis. J. Affect. Disord. 190, 264–271. https://doi.org/10.1016/j.jad.2015.09.069.
Zou, J., Tao, S., Johnson, A., Tomljanovic, Z., Polly, K., Klein, J., Razlighi, Q.R., Brickman, A.M., Lee, S., Stern, Y., Kreisl, W.C., 2020. Microglial activation, but not tau pathology, is independently associated with amyloid positivity and memory impairment. Neurobiol. Aging 85, 11–21. https://10.1016/j.neurobiolaging.2019.09.019.